



Cite this: DOI: 10.1039/c8nj01248b

# Synthesis, photophysical, antibacterial and larvicidal studies on triazolophanes with 5-nitro isophthalate functionality at the intraannular position†

Sivasamy Selvarani,<sup>a</sup> Perumal Rajakumar,<sup>ib</sup>\*<sup>a</sup> Subramani Nagaraj,<sup>b</sup> Manisha Choudhury<sup>c</sup> and Devadasan Velmurugan<sup>c</sup>

1:1 and 2:2 oligomeric triazolophanes with 5-nitro isophthalate and triazolyl functionalities at the intraannular position have been synthesized by copper(I) catalyzed 1,3 dipolar cycloaddition of the corresponding propargylic esters with various phenyl substituted aliphatic azides under mild conditions through click methodology. The 1:1 oligomeric triazolophanes exhibit good target binding ability and better antibacterial activity against *Staphylococcus aureus*, *Bacillus subtilis*, *Salmonella typhi* and *Escherichia coli* bacteria than the 2:2 oligomeric triazolophanes, supported by molecular docking studies, and triazolophanes **T3**, **T4** and **T5** show good larvicidal activity.

Received 13th March 2018,  
Accepted 19th June 2018

DOI: 10.1039/c8nj01248b

rsc.li/njc

## Introduction

Over the past few decades, the synthesis of bioactive macrocycles with 1,2,3-triazole ring systems has generated great interest from researchers due to their excellent optoelectronic and biological activities.<sup>1</sup> Triazolophane motifs can be embedded between two or more active residues, which can function as multiple targets due to their improved lipophilicity, membrane penetration, metabolic stability, solubility, and oral bioavailability.<sup>2,3</sup> Triazole containing macrocycles exhibit various applications in many fields such as host–guest complexation, molecular recognition,<sup>4</sup> antibacterial,<sup>5</sup> antifungal,<sup>6</sup> antiviral, anti-inflammatory, anti-cancer,<sup>7</sup> larvicidal<sup>8a</sup> and antimalarial activities.<sup>8b</sup>

Triazoles can function as biological linkers and as bridging units in supramolecular architectures which exhibit chemical stability under physiological conditions.<sup>9</sup> Moreover, triazoles play a crucial role in the field of pharmaceutical chemistry because of their ability to form hydrogen bonding, which is essential for their solubility and biological activity.<sup>10</sup> Triazoles can be generated by click methodology which is highly reliable,

simple and regioselective.<sup>11</sup> Click chemistry<sup>12</sup> has been extensively applied in many fields such as antibacterial polymers,<sup>13</sup> dyes,<sup>14</sup> corrosion inhibitors,<sup>15</sup> drugs,<sup>16</sup> photo stabilizers<sup>17</sup> and photographic materials. The synthesis of supramolecular architectures such as dendrimers<sup>18</sup> and cyclophanes<sup>19</sup> with a triazole unit is of interest due to their biological applications. Macrocycles having ester and phenolic functionalities show antibacterial,<sup>20</sup> antioxidant and larvicidal activity. Moreover, some of the ester macrocycles show larvicidal activity against the larvae of *Aedes aegypti* mosquitoes.<sup>21</sup>

Though naturally occurring<sup>22</sup> and synthetic<sup>23</sup> aromatic esters are used as fragrant materials, such as fructose and ethyl methyl phenyl glycidate, they are also used as drug materials, such as benzyl benzoate, pivampicillin *etc.*

The biological significance of aromatic nitroesters with triazole functionality prompted us to synthesize the new class of triazolophanes **1–10** (Fig. 1) and explore their photophysical, antibacterial and larvicidal activity.

## Result and discussion

### Triazole based macrocycles

Triazole based macrocycles **1–10** (Fig. 1) can be synthesized from the corresponding bispropargyloxy ester functionalized precyclophane. The required bispropargyloxy precyclophanes can be obtained from 5-nitro isophthalic acid and propargyl alcohol. Click reaction is a novel approach for the synthesis of prospective drugs from alkynes and azides. From this point of view, we have synthesized the ester based triazolophanes **1–10**,

<sup>a</sup> Department of Organic Chemistry, University of Madras, Maraimalai (Guindy) Campus, Chennai–600 025, India. E-mail: perumalrajakumar@gmail.com; Fax: +91 44 235 2494; Tel: +91 44 22202810

<sup>b</sup> Centre for Advanced Studies in Botany, University of Madras, Maraimalai (Guindy) Campus, Chennai–600 025, India

<sup>c</sup> CAS in Crystallography and Biophysics, University of Madras, Maraimalai (Guindy) Campus, Chennai–600 025, India

† Electronic supplementary information (ESI) available. See DOI: 10.1039/c8nj01248b

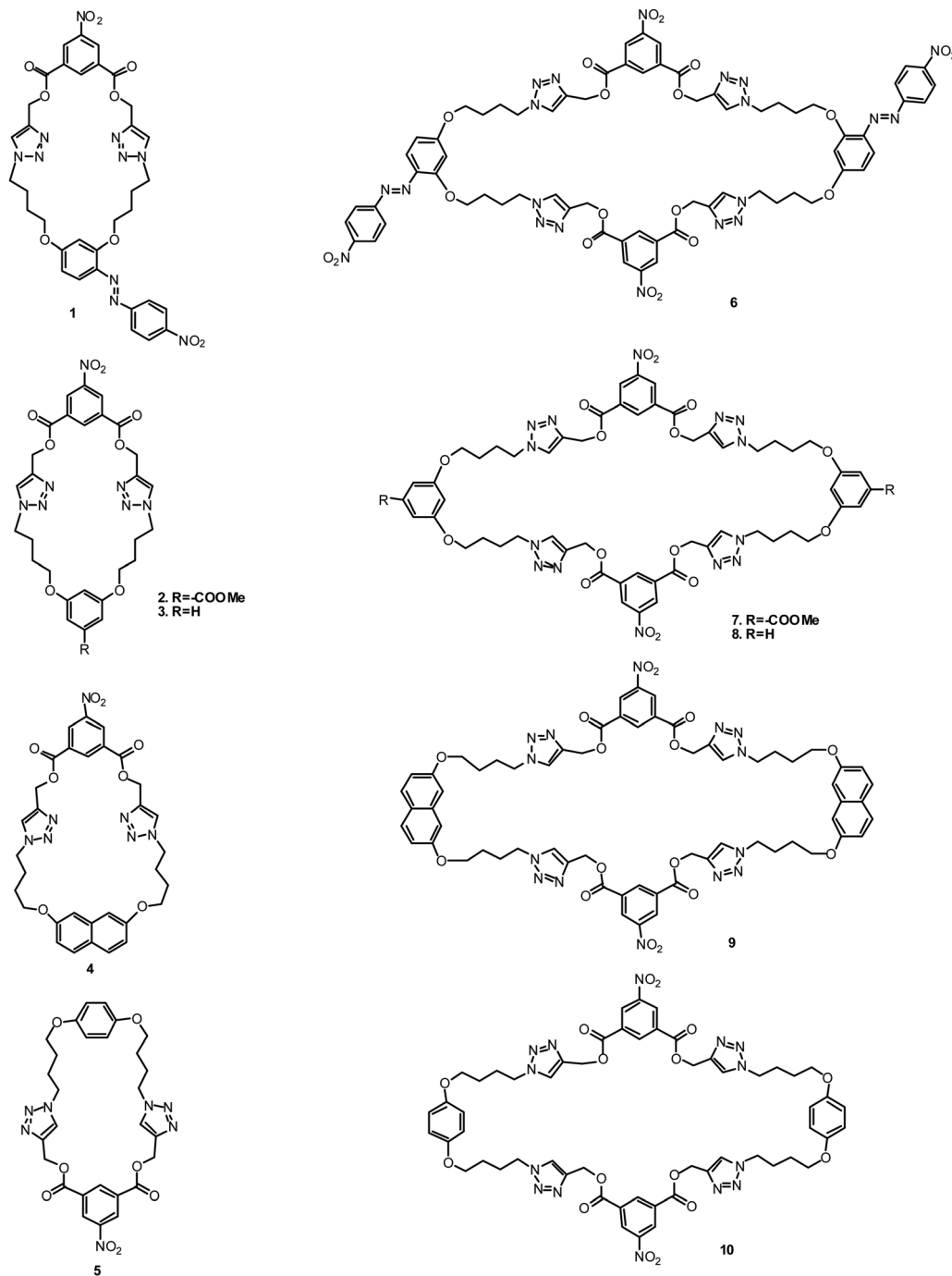


Fig. 1 Molecular structure of 1:1 (1–5) and 2:2 (6–10) oligomeric triazolophanes.

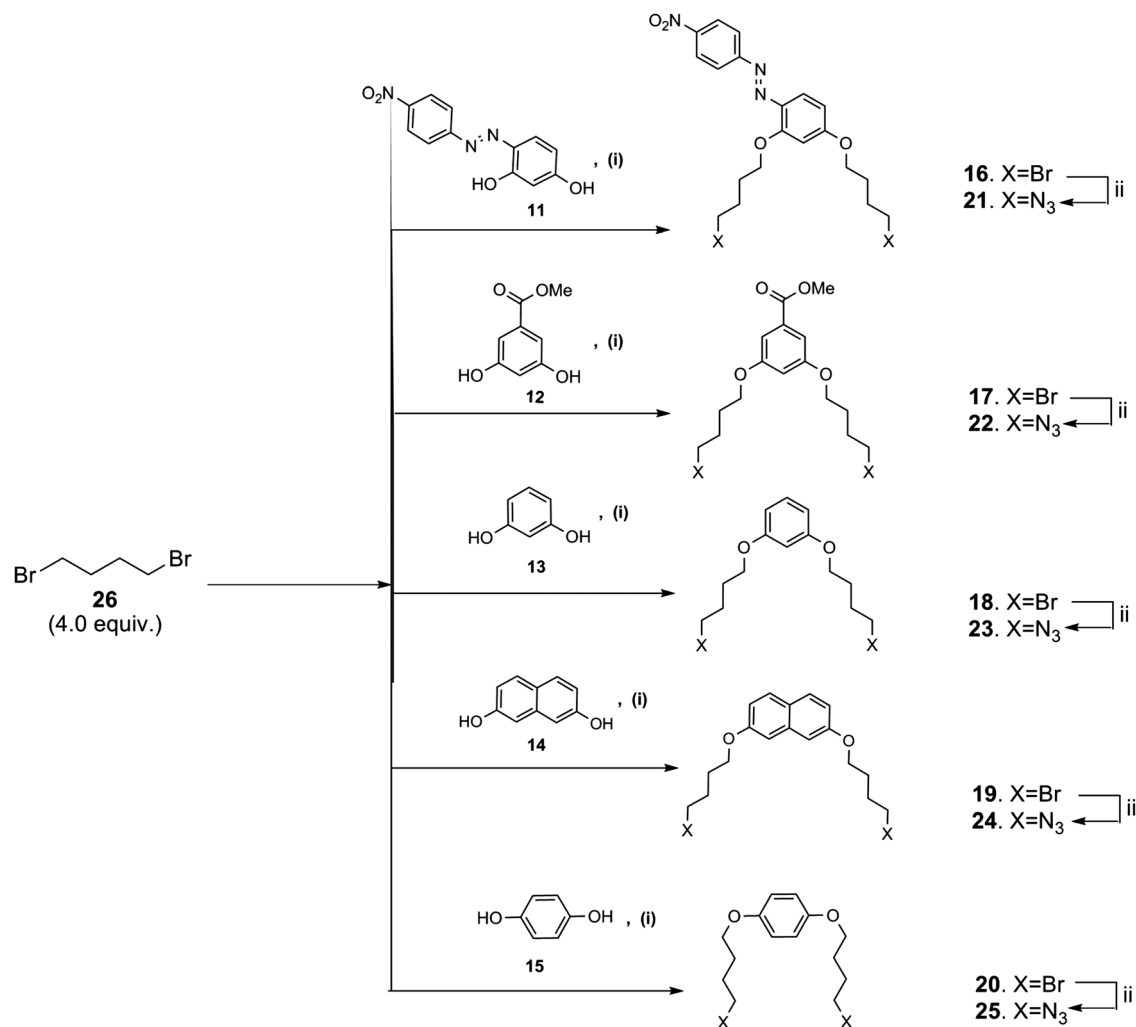
from the bispropargyloxy precyclophane esters and the corresponding aryl alkyl azides **21**, **22**, **23**, **24** and **25**, which in turn can be obtained from the corresponding bisbromides and sodium azide.

#### Synthesis and characterization of the triazolophanes

The bisbromides **16**, **17**, **18**, **19** and **20** were obtained in 69%, 79%, 72%, 78% and 75% yields, respectively by the reaction of 1.0 equiv. of each of the diols *viz* *E*-4-((4-nitrophenyl)diazanyl)benzene-1,3-diol **11**, methyl 3,5-dihydroxybenzoate **12**, Resorcinol **13**, naphthalene-

2,7-diol **14**, and 1,4-dihydroxybenzene **15** with 4.0 equiv. of 1,4-dibromobutane **26** in acetone and in the presence of 3.0 equiv. potassium carbonate at 60 °C for 7 h (Scheme 1).

The <sup>1</sup>H NMR spectrum of *E*-1-(2,4-bis(4-bromobutoxy)phenyl)-2-(4-nitrophenyl)diazene **16** showed bromomethylene and *O*-methylene protons as a triplet at  $\delta$  3.51 and 3.58, and 4.09 and 4.23 in addition to the signals for the other aliphatic and aromatic protons. The <sup>13</sup>C NMR spectrum of *E*-1-(2,4-bis(4-bromobutoxy)phenyl)-2-(4-nitrophenyl)diazene **16** displayed signals for the bromomethylene and *O*-methylene carbons



**Scheme 1** Reagents and conditions: (i)  $\text{K}_2\text{CO}_3$  (3.0 equiv.), acetone (dry), 12 h. **16** (69%); **17** (79%); **18** (72%); **19** (78%); **20** (75%). (ii)  $\text{NaN}_3$  (2.2 equiv.), acetone :  $\text{H}_2\text{O}$  (3 : 1, 40 mL), 60 °C, 12 h. reflux. **21** (77%); **12** (79%); **13** (71%); **14** (75%); **25** (81%).

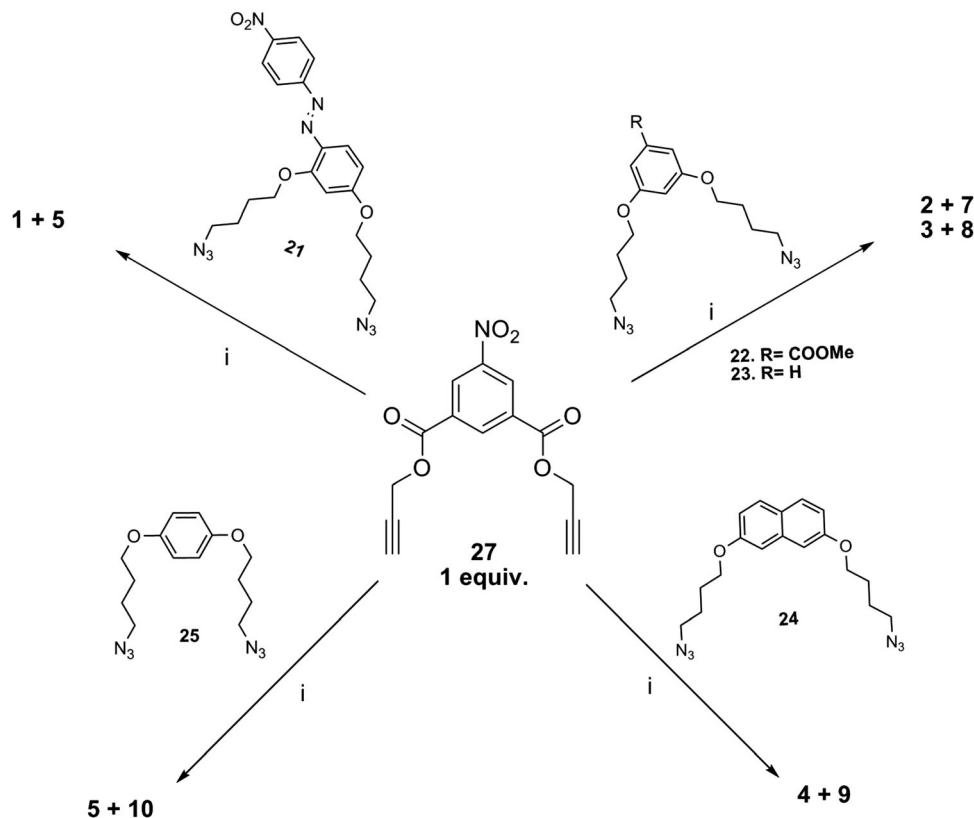
at  $\delta$  33.2, 33.5 and 67.4, 68.7 in addition to the signals of the two aliphatic carbons and ten aromatic carbons. In the mass spectrum the appearance of a molecular ion peak at  $m/z$  527 [ $\text{M}^+$ ] also confirmed the structure of *E*-1-(2,4-bis(4-bromobutoxy)phenyl)-2-(4-nitrophenyl)diazene **16**. Furthermore, the elemental analysis also supported the composition of *E*-1-(2,4-bis(4-bromobutoxy)phenyl)-2-(4-nitrophenyl)diazene **16**.

Similarly, the structure of the bisbromides **17**, **18**, **19** and **20** was also confirmed from spectral and analytical data. The reaction of 1.0 equiv. of each of the bisbromides **16**, **17**, **18**, **19** and **20** with 2.2 equiv. of sodium azide in acetone : water (3 : 1, 40 mL) at 60 °C for 12 h afforded the corresponding aryl alkyl azides **21**, **22**, **23**, **24** and **25** in 77%, 79%, 71%, 75% and 81% yields, respectively (Scheme 1).

In the  $^1\text{H}$  NMR spectrum *E*-1-(2,4-bis(4-azidobutoxy)phenyl)-2-(4-nitrophenyl)diazene **21** showed azidomethylene and *O*-methylene protons as triplets at  $\delta$  3.32 and 3.35, and 4.01 and 4.14 in addition to the signals for the other aliphatic and aromatic protons. The  $^{13}\text{C}$  NMR spectrum of *E*-1-(2,4-bis(4-azidobutoxy)phenyl)-2-(4-nitrophenyl)diazene **21** displayed

signals for the azidomethylene and *O*-methylene carbons at  $\delta$  55.4, 55.8 and 65.4, 65.9 in addition to the signals for the other aliphatic carbons and for the ten aromatic carbons. In the mass spectrum the appearance of the molecular ion peak at  $m/z$  453 [ $\text{M}^+$ ] also confirmed the structure of *E*-1-(2,4-bis(4-azidobutoxy)phenyl)-2-(4-nitrophenyl)diazene **21**. Furthermore, the elemental analysis also supported the composition of *E*-1-(2,4-bis(4-azidobutoxy)phenyl)-2-(4-nitrophenyl)diazene **21**. Similarly, the structure of the bisazides **22**, **23**, **24** and **25** was also confirmed from spectral and analytical data as shown in the ESI $^+$  (Fig. S5, S6, S9, S10, S13 and S14).

The synthesis of the ester based 1:1 oligomeric triazolophanes **1**, **2**, **3**, **4** and **5** and 2:2 oligomeric triazolophanes **6**, **7**, **8**, **9** and **10** is shown in Scheme 2. The reaction of 4.0 equiv. of propargyl alcohol with one equiv. of 5-nitroisophthaloyl chloride afforded the precyclophane ester **27** as reported earlier from our laboratory.<sup>20</sup> The reaction of 1.0 equiv. of bispropargyl-5-nitroisophthalate **27** with 1.0 equiv. of each of the bisazides **21**, **22**, **23**, **24** and **25** in the presence of  $\text{CuSO}_4 \cdot 5\text{H}_2\text{O}$  (10 mol%), sodium ascorbate (10 mol%) in a mixture of THF-water (3 : 1) at room



**Scheme 2** Reagents and conditions: (i)  $\text{CuSO}_4 \cdot 5\text{H}_2\text{O}$  (10 mol%), sodium ascorbate (10 mol%)  $\text{THF-H}_2\text{O}$  (3 : 1), rt, 12 h. **1** (32%); **2** (25%); **3** (38%); **4** (29%); **5** (32%); **6** (30%); **7** (28%); **8** (30%); **9** (25%); **10** (33%).

temperature for 12 h afforded the corresponding 1 : 1 triazolophanes **1**, **2**, **3**, **4** and **5** in 32%, 25%, 38%, 27% and 32% yields and the same reaction also provided the 2 : 2 oligomeric triazolophanes **6**, **7**, **8**, **9** and **10** in 30%, 28%, 30%, 25% and 33% yields, respectively (Scheme 2). The 1 : 1 and 2 : 2 oligomeric triazolophanes can be easily separated by column chromatography on silica gel with  $\text{CHCl}_3$ :methanol (3 : 1) as the eluent for 1 : 1 and  $\text{CHCl}_3$ :methanol (4 : 1) as the eluent for 2 : 2 oligomeric triazolophanes.

The  $^1\text{H}$  NMR spectrum of 1 : 1 oligomeric ester functionalized triazolophane **1** displayed two sharp singlets at  $\delta$  1.85, 2.09 for aliphatic protons, the *O*-methylene protons appeared as a singlet at  $\delta$  4.43, 5.49, the *N*-methylene protons appeared as a doublet at  $\delta$  4.05, and the triazole proton appeared as a singlet at  $\delta$  7.66 in addition to the signals for the aromatic protons. The  $^{13}\text{C}$  NMR spectrum of the 1 : 1 oligomeric triazole macrocycle **1** showed five signals at  $\delta$  24.8, 26.4, 58.1, 66.5 and 68.2 for the aliphatic methylene, *N*-methylene, and *O*-methylene carbons and the triazolyl carbon appeared at  $\delta$  127.7 in addition to the signals for the aromatic carbons. From the appearance of a molecular ion peak at  $m/z$  741  $[\text{M} + \text{H}^+]$  and also from the elemental analysis the structure of the macrocyclic ester **1** was confirmed. Similarly, the structure of the 1 : 1 oligomeric triazole macrocycles **3**, **4** and **5** was confirmed from spectral and analytical data as shown in the ESI $^\dagger$  (Fig. S15).

The  $^1\text{H}$  NMR spectrum of 2 : 2 oligomeric triazolophane **6** showed a triplet at  $\delta$  4.02, 4.16 for the eight protons of the

*N*- $\text{CH}_2$ , the *O*- $\text{CH}_2$  protons appeared as a triplet at  $\delta$  4.52, 4.56, and the triazolyl proton appeared as a singlet at 7.78, in addition to the signals for aromatic protons. The  $^{13}\text{C}$  NMR spectrum of the 2 : 2 oligomeric triazolophane **6** showed signals at  $\delta$  26.0, 27.0, 50.1, 59.0, 67.4, 68.7 and 128.4 for aliphatic methylene, *N*-methylene, *O*- $\text{CH}_2$  and triazole carbon, in addition to the other signals for the aromatic carbons. The mass spectrum of the 2 : 2 oligomeric triazolophane **6** showed the molecular ion peak at  $m/z$  1481  $[\text{M} + \text{H}^+]$ . Similarly, the structure of the 2 : 2 oligomeric cyclophane esters **7**, **8**, **9** and **10** was characterized from spectral and analytical data as shown in the ESI $^\dagger$  (Fig. S16).

### Photophysical studies on the 1 : 1 and 2 : 2 oligomeric triazolophanes

The UV-vis absorption spectra of triazolophanes **1-10** were recorded in DCM at a concentration of  $1 \times 10^{-5}$  M and the  $\lambda_{\text{max}}$  values are summarized in Table 1. All the triazolophanes showed two absorption bands between 239 and 399 nm in the absorbance spectrum (Fig. 2a and b) except for the cyclophanes **4** and **9** which showed an absorbance band at 241–242 nm. The absorption maximum between 239 and 251 nm for all the cyclophanes could be due to the  $\pi$ - $\pi^*$  transition and the absorption maximum at higher wavelengths between 289 and 399 nm could be due to the  $n$ - $\pi^*$  transition. However, the triazolophanes **1** and **6** showed a strong absorption band

**Table 1** UV-Vis spectral data of the nitroester based triazolophanes **1–10**

Triazolophanes	$\lambda_{\text{abs max}}$ (nm)	O.D.	$\epsilon$ (mol L <sup>-1</sup> cm <sup>-1</sup> ) $\times 10^5$
<b>1</b>	239, 397	0.43, 0.54	4.3, 5.4
<b>2</b>	242, 291	1.57, 0.55	1.6, 5.5
<b>3</b>	251, 306	1.35, 0.36	1.4, 3.6
<b>4</b>	241	0.70	7.0
<b>5</b>	242, 295	0.75, 0.23	7.5, 2.3
<b>6</b>	242, 399	0.74, 0.95	7.4, 9.5
<b>7</b>	241, 289	1.95, 0.66	1.9, 6.6
<b>8</b>	251, 305	1.74, 0.43	1.7, 4.3
<b>9</b>	242	1.05	1.1
<b>10</b>	241, 306	1.02, 0.27	1.0, 2.7

between 397 and 399 nm assigned to the n- $\pi^*$  transitions of the azobenzene chromophore.

### Photoisomerisation studies

The azobenzene chromophore shows photoinduced, reversible *cis/trans* isomerisation. The photoinduced *trans* to *cis* isomerisation behavior of dendrimers **1** and **6** was investigated by UV-vis spectrophotometry. The triazolophanes **1** and **6** were irradiated at 365 nm to induce *trans-cis* isomerisation. Fig. 3 shows the photoisomerisation of triazolophane **1** on UV irradiation. Photo irradiation of the azodendrimers at the concentration of  $1 \times 10^{-5}$  M using 365 nm in CHCl<sub>3</sub> results in a decrease in the intensity of the absorbance at 398 nm and increases the intensity of the band at 318 nm, which is assigned to *trans-cis* photoisomerisation.

Triazolophane **1** undergoes *trans-cis* isomerisation as revealed by the decrease in the absorbance for the *trans* isomer and increase in the absorbance of the *cis* isomer. The isosbestic point was observed at 318 nm and the system needs 12 minutes to attain the photostationary state.

### Antibacterial activity

Bacterial infection is a worldwide health issue due to the resistance of microorganisms to the existing drugs. Hence, there is an urgent need to find new antibacterial drugs which would exhibit bactericidal and bacteriostatic activity. The synthetic

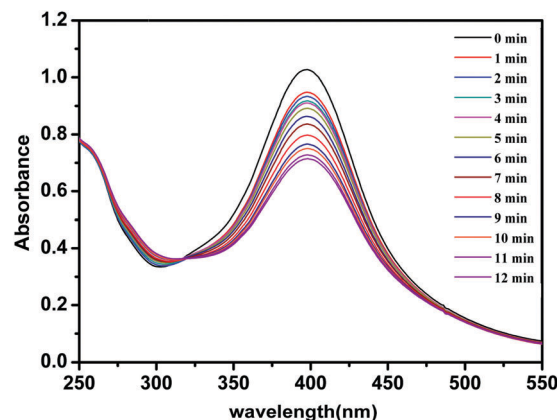


**Fig. 3** Photoisomerisation of triazolophane **1** irradiated at 365 nm by a UV lamp in CHCl<sub>3</sub> ( $1 \times 10^{-5}$  M) solution.

antibacterial agents are better than the natural ones because of the possibility to overcome the drug resistance and improve the antibacterial activity by structural modifications. Ester based piperazinophanes against *Escherichia coli*, *Klebsiella pneumoniae*, *Staphylococcus aureus* and *Staphylococcus pyogens* bacteria have been reported from our laboratory earlier<sup>20</sup> and the reported piperazinophanes have shown remarkable antibacterial activity against *Escherichia coli* and *Staphylococcus aureus*. Ester functionalized 1,4-disubstituted 1,2,3-bistriazole<sup>24</sup> shows good antibacterial activity against *Escherichia coli*. The *in vitro* antibacterial activity of the synthesized novel triazole based cyclophanes T1 (triazolophane **1**) to T10 (triazolophane **10**) was screened by a well diffusion assay.<sup>25</sup> The four test bacterial strains *Staphylococcus aureus* (MTCC96), *Bacillus subtilis* (MTCC441), *Salmonella typhi* (ATCC 6539) and *Escherichia coli* (MTCC 1698) were selected for the antibacterial activity study and compared with commercial antibiotic cefotaxime. Table 2 shows the diameter of the zone of inhibition around the disk expressed in millimeters (mm) for all synthesized triazolophanes **1–10** against the bacterial strains with tetracycline as the standard. Triazolophanes T3 and T5 showed the highest inhibition zones for both

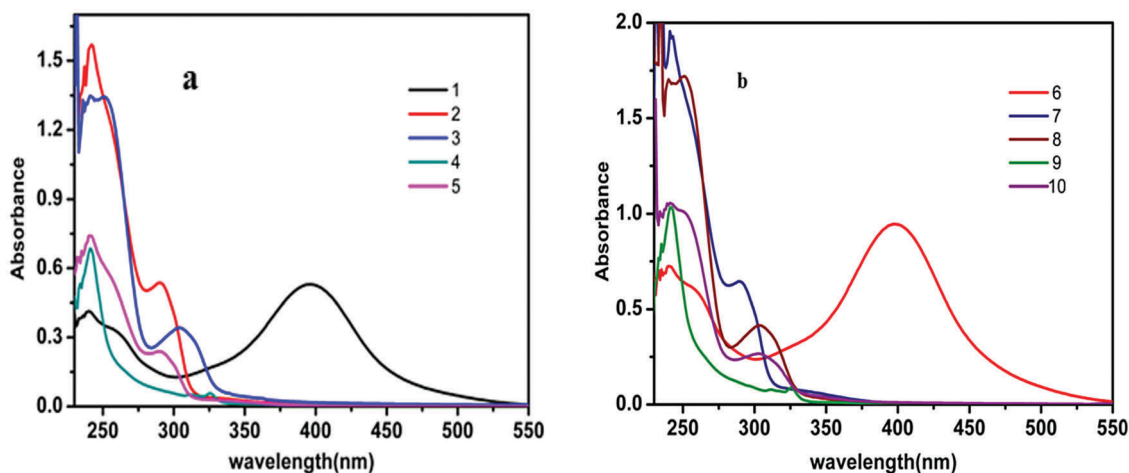


**Fig. 2** UV-Vis spectra of (a) 1:1 oligomers **1–5** and (b) 2:2 oligomers **6–10** at a concentration of  $1 \times 10^{-5}$  in dichloromethane at room temperature.

**Table 2** *In vitro* antibacterial activity of the synthesized triazolophanes **1–10** at 50, 75 and 100  $\mu\text{g mL}^{-1}$  by well diffusion assay

Triazolophanes	Zone of inhibition (mm)															
	Gram positive bacteria								Gram negative bacteria							
	<i>Staphylococcus aureus</i> (MTCC96)				<i>Bacillus subtilis</i> (MTCC441)				<i>Salmonella typhi</i> (ATCC6539)				<i>Escherichia coli</i> (MTCC1689)			
	A	b	c	d	a	b	c	d	a	b	c	d	a	b	c	d
<b>1</b>	12	15	16	17	10	11	12	29	13	16	15	18	10	12	13	19
<b>2</b>	—	10	13	15	12	13	15	24	—	—	15	17	—	12	14	20
<b>3</b>	16	17	21	23	19	21	24	27	17	19	21	24	13	15	17	22
<b>4</b>	—	13	15	19	10	14	17	20	—	10	12	20	—	—	—	23
<b>5</b>	17	19	22	25	17	23	25	29	19	21	24	26	10	13	15	24
<b>6</b>	12	13	15	17	13	11	15	17	—	—	10	18	—	—	12	19
<b>7</b>	—	9	11	13	11	15	17	29	—	9	14	15	—	7	12	20
<b>8</b>	—	7	8	15	12	14	18	28	—	—	11	13	—	—	12	19
<b>9</b>	—	—	11	13	10	12	15	24	—	—	9	12	—	—	12	20
<b>10</b>	12	13	14	19	10	11	14	22	—	—	13	18	—	—	12	14
Control	—	—	—	—	—	—	—	—	—	—	—	—	—	—	—	—

Note: *a* = 50  $\mu\text{g mL}^{-1}$  of sample; *b* = 75  $\mu\text{g mL}^{-1}$  of sample; *c* = 100  $\mu\text{g mL}^{-1}$  of sample; *d* = standard drug (30  $\mu\text{g mL}^{-1}$  of cefotaxime).

Gram positive and Gram negative pathogenic bacteria compared to **T1**, **T2** and **T4**. The 2:2 oligomeric triazolophane **T6** showed better antimicrobial activity towards the Gram positive microorganisms, *viz.* *Staphylococcus aureus* (MTCC96) and *Bacillus subtilis* (MTCC441), than the Gram negative bacteria, *viz.* *Escherichia coli* (MTCC 1698) and *Salmonella typhi* (ATCC 6539). The triazole based 2:2 oligomeric cyclophanes **T7**, **T8**, **T9** and **T10** also inhibited the antibacterial activity to some extent in most of the tested concentrations. In conclusion, all the synthesized compounds particularly **T3**, **T4**, **T5** and **T6** have increased antibacterial activity against all the selected human pathogenic bacteria. The triazolophanes **T3**, **T4**, **T5** and **T6** may be developed further as antibacterial drugs as they exhibit better antibacterial activity against the tested pathogens than all the other compounds including cefotaxime. However, further studies are required to determine their mode of action and their potential application against a wide range of human pathogens. Dimethyl sulfoxide was used as the control which showed nil activity with reference to all the tested bacteria.

### Molecular docking

The molecular docking study was carried out to analyze the binding affinity of the test compounds with the target protein CTXM-enzyme in complex with cefotaxime (PD ID: 3HLW). In Gram-negative bacteria, the production of  $\beta$ -lactamases is the main cause of resistance to  $\beta$ -lactam antibiotics.  $\beta$ -Lactamases cleave the amide bond in the  $\beta$ -lactam ring and makes  $\beta$ -lactam antibiotics harmless to bacteria (Julien Delmas, *et al.*, 2010). Consequently, the CTXM-family calls for attention for the design of inhibitors.

**Table 3** Glide score and glide energy of compounds **T2**, **T3**, **T4** and **T5**

Triazolophanes	Glide score	Glide energy, kcal mol <sup>-1</sup>
<b>T4</b>	-3.52	-31.92
<b>T5</b>	-3.41	-34.67
<b>T2</b>	-2.55	-40.70
<b>T3</b>	-3.42	-34.80

From GLIDE XP docking, out of ten ligands, only four ligands **T2**, **T3**, **T4** and **T5** showed interaction with the target protein (Table 3). The remaining compounds did not show encouraging results in docking due to the incompatibility of the structures with the active site. Furthermore, an induced fit docking study was carried out for the compounds **T3** and **T5** which showed comparable glide energy and docking score to the reference inhibitor cefotaxime (Table 4). The compounds show a considerable number of both hydrogen bond and hydrophobic interactions with the active site residues.

Compound **T3** showed interactions with the key residues Asn104 and Asn132 with a binding energy of  $-46.05$  kcal mol<sup>-1</sup> and a glide score of  $-5.27$  in comparison with cefotaxime with a binding energy of  $-69.33$  kcal mol<sup>-1</sup> and glide score of  $-8.07$  kcal mol<sup>-1</sup> respectively as evident from Fig. 4. The compound **T5** showed hydrogen bond interaction with the residues Asn132 and Asn104 with a glide score of  $-4.74$  and glide energy of  $-52.30$  kcal mol<sup>-1</sup> as shown in the ESI.†

### Structure activity relationship studies

Based on the structure of the triazolophanes the *in vitro* antibacterial activity revealed that the triazolophanes **T2**, **T3** and **T5** having triazoles with ester moieties show better activity as compared to the other cyclophanes as they can interact with bacteria through van der Waals and hydrophobic interactions. Moreover, 1,2,3-triazole has rigidifying nature, which can improve their

**Table 4** Induced fit docking results of compounds **T3**, **T5** and cefotaxime at the substrate binding site

Triazolophanes	Glide score	Glide energy, kcal mol <sup>-1</sup>	Hydrogen bond	
			D-H...A	Distance (Å)
<b>T3</b>	-5.27	-46.05	Ans104 N-H...O	3.26
			Ans132 N-H...O	3.06
<b>T5</b>	-4.74	-52.30	Ans132 N-H...O	3.01
			Thr235 O-H...O	3.01
Cefotaxime (co-crystal)	-8.07	-69.33	Asn132 N-H...O	3.01
			Asn104 N-H...O	3.00

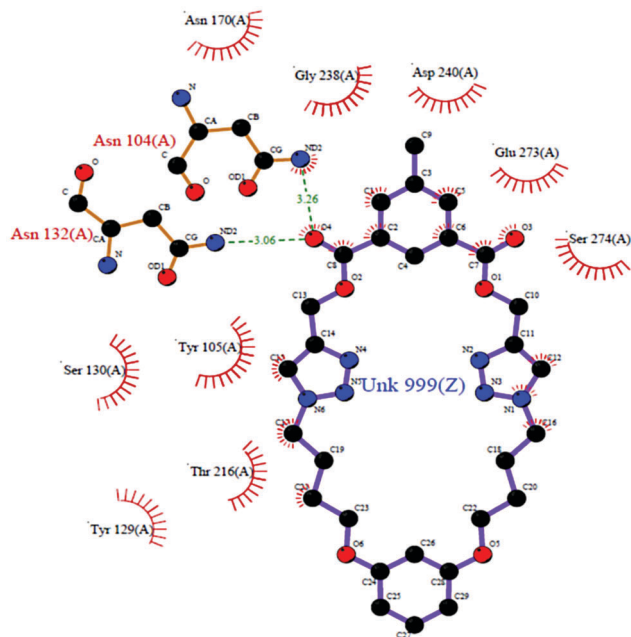


Fig. 4 Molecular docking of compound T3 in the active pocket of protein CTXM (PDBID-3HLW).

affinity to the target proteins. The electron donating triazole and oxygen present in the structure could interact by hydrogen bonding on the macrocycles and enhanced the antibacterial activity. Among the 1 : 1 and 2 : 2 oligomeric triazolophanes the inhibition activity depends on the nature of the substituents. Triazolophane T6 showed moderate activity because of the azobenzene along with a triazole unit in the macrocycles. The triazolophane T7 showed better activity than all other triazolophanes due to the electron withdrawing groups, such as nitro and ester groups, present in the *p*-position of the intra annular position. The 1 : 1 oligomers (1–5) showed better antibacterial activity than the 2 : 2 oligomers (6–10) because of their high solubility in polar solvents, and hence they can be easily applied to a substrate, and they also have aliphatic chain. Thus, the nature of the aromatic unit with an ester and triazole skeleton attached to phenoxy molecules has a strong influence on the extent of antibacterial activity.

### Larvicidal activity

Mosquitoes act as a vector for many subtropical and tropical diseases which are very harmful to humans. The mosquito spreads diseases such as chikunguniya, dengue fever, dengue hemorrhagic fever and yellow fever. Among these common diseases, dengue hemorrhagic fever is highly fatal and it is transmitted through the vector *Aedes aegypti*. The WHO estimates that there may be nearly 50 million people affected by dengue fever worldwide every year. The vaccine for this virus is still at an early stage and therefore the only available method to reduce the disease infection is by controlling the vector. The vectors can be controlled either by killing, preventing the mosquitoes from biting humans and causing mortality to the mosquito larvae on a large scale. New approaches are needed for the control of these vectors. The cyclophanes and

dendrimers are already reported to possess a variety of biological functions and an attempt to evaluate their larvicidal activity was carried out.

The larvicidal activity was determined according to the WHO (World Health Organization) protocol<sup>26</sup> with slight modification. The test compounds were dissolved in 10  $\mu\text{L}$  of DMSO due to its solubility in water. The mosquito larvae were treated with the compounds at a concentration of 2000  $\mu\text{g mL}^{-1}$ . The larvae treated with DMSO were maintained as a control. The mortality of fourth instar larvae of *Aedes aegypti* was observed and the number of surviving larvae at the end of 24 and 48 hours was observed. The percentage of mortality was calculated using the below formula:

$$\text{Percentage of mortality} = \left( \frac{\text{No. of larva dead}}{\text{No. of larvae introduced}} \right) \times 100$$

The larvae treated with the test compounds showed significant behavioral changes which include restlessness, loss of equilibrium and finally death. The percentage of mortality varies among the compounds tested. The high mortality percentage of 90% was observed in larvae treated with triazolophane T5 followed by compounds T3 and T4 with 80% mortality each. Among the synthesized triazolophanes T6, T7, T8, T9 and T10 show low mortality percentage. Triazolophanes T1, T2 and T3 show moderate mortality percentage when compared with the other triazolophanes. The results are tabulated in Table 5.

In conclusion, ester based 1 : 1 and 2 : 2 oligomeric triazolophanes 1–10 have been successfully achieved under mild conditions. Nitroarene substituted triazolophanes 1 and 6 showed a strong absorption band between 397 and 399 nm assigned to  $n-\pi^*$  transitions of the azobenzene chromophore. *In vitro* antibacterial studies and molecular docking analysis of the compounds against four human pathogens *Staphylococcus aureus* (MTCC96), *Bacillus subtilis* (MTCC441), *Salmonella typhi* (ATCC 6539) and *Escherichia coli* (MTCC 1698) revealed that triazolophanes T3 and T5 exhibited better antibacterial activity than the other triazolophanes. All the 1 : 1 oligomeric triazolophanes show better antibacterial activity against *Staphylococcus aureus* (MTCC96), *Bacillus subtilis* (MTCC441), *Salmonella typhi*

Table 5 Larvicidal activity of the synthesized triazolophanes 1–10 at 2000  $\mu\text{g mL}^{-1}$  by larvicidal activity assay

Larvae	Triazolophanes	Mortality percentage (%)
4th instar larvae <i>Aedes aegypti</i>	T1	50
	T2	70
	T3	80
	T4	80
	T5	90
	T6	60
	T7	30
	T8	30
	T9	40
	T10	30
	Control (DMSO)	0

(ATCC 6539) and *Escherichia coli* (MTCC 1698) than the 2:2 oligomeric triazolophanes. The triazolophanes T3 and T5 may prove to be potential structural scaffolds for designing anti-bacterial drugs among all the synthesized compounds, and triazolophane T5 showed the best larvicidal activity among all the tested triazolophanes.

## Conflicts of interest

There are no conflicts to declare.

## Acknowledgements

The authors acknowledge UGC, New Delhi, India for financial support and DST, New Delhi for the NMR facility under the DST-FIST programme to the Department of Organic Chemistry, University of Madras. SS thanks DST PURSE Phase II for providing a fellowship in the form of a JRF.

## Notes and references

- J. H. Mohammed, I. A. Mohammed and S. J. Abass, *J. Chem. Sci.*, 2015, **5**, 317.
- A. Lauria, R. Delisi, F. Mingoia, A. Terenzi, A. Martorana, G. Barone and A. M. Almerico, *Eur. J. Org. Chem.*, 2014, 3289.
- Y. Xufen and S. Dianqing, *Molecules*, 2013, **18**, 6230.
- V. Haridas, S. Sahu, P. Praveen Kumar and A. R. Sapala, *RSC Adv.*, 2012, **2**, 12594–12605.
- J. A. Demaray, J. E. Thuener, M. N. Dawson and S. J. Sucheck, *Bioorg. Med. Chem. Lett.*, 2008, **18**, 4868.
- M. Gaur, M. Goel, L. Sridhar, T. D. S. Ashok, S. Prabhakar, P. Dureja, P. Raghunathan and S. V. Eswaran, *Monatsh. Chem.*, 2012, **143**, 283.
- J. L. Yu, Q. P. Wu, Q. S. Zhang, Y. H. Liu, Y. Z. Li and Z. M. Zhou, *Bioorg. Med. Chem. Lett.*, 2010, **20**, 240.
- (a) J. W. Zhang, Z. Hu, P. Gao, J. R. Wang, Z. N. Hu and J. W. Wu, *Int. J. Mol. Sci.*, 2013, **14**, 24064–24073; (b) J. H. Mohammed, I. A. Mohammed and J. S. Abass, *J. Chem. Sci.*, 2015, **6**, 317.
- K. Bebenek, M. Jastrzebska, M. Kadela-Tomanek, E. Chrobak, B. Orzechowska, K. Zwolinska, M. Latocha, A. Mertas, Z. Czuba and S. Boryczka, *Molecules*, 2017, **11**, 1876.
- D. Dheera, V. Singh and R. Shankar, *Bioorg. Chem.*, 2017, **71**, 30–54.
- D. Pasini, *Molecules*, 2013, **18**, 9512.
- A. Ta ba caru, B. Furdui, I. O. Ghinea, G. Carac and R. M. Dinica, *Inorg. Chem. Acta*, 2017, **455**, 329.
- C. N. Urbani, C. A. Bell, M. R. Whittaker and M. J. Monteiro, *Macromolecules*, 2008, **41**, 1057.
- R. A. Turner, A. G. Oliver and R. S. Lokey, *Org. Lett.*, 2007, **9**, 5011.
- J. Totobenazara and A. J. Burke, *Tetrahedron Lett.*, 2015, **56**, 2853.
- D. Dheer, V. Singh and R. Shankar, *Bioorganic Chemistry*, 2017, **71**, 30–54.
- X. L. Zhao, K. F. Yang, Y. Zhang, L. W. Xu and X. Q. Guo, *Catal. Commun.*, 2016, **74**, 110.
- V. Saravanan, A. Kannan and P. Rajakumar, *New J. Chem.*, 2017, **41**, 1714.
- R. Anandhan, A. Kannan and P. Rajakumar, *Synth. Commun.*, 2016, **47**, 671.
- S. Selvarani and P. Rajakumar, *New J. Chem.*, 2016, **40**, 9494.
- R. Pavela, *Ind. Crops Prod.*, 2015, **76**, 174.
- S. A. A. G. Almeida, A. C. Meneses, P. H. Hermes de Araujo and D. Oliveira, *Trends Food Sci. Technol.*, 2017, **69**, 95.
- M. Wang, Z. Wu, W. Qi and R. Su, *J. Mol. Catal. B: Enzym.*, 2014, **110**, 32.
- K. Lal, A. Kumar, M. S. Pavan and C. P. Kaushik, *Bioorg. Med. Chem. Lett.*, 2012, **22**, 4353–4357.
- J. L. Rios, M. C. Recio and A. Villar, *J. Ethnopharmacol.*, 1988, **23**, 127.
- World Health Organization, Instructions for determining the susceptibility or resistance of mosquito larvae to insecticides, WHO/VBC, 1981, **81**, 807.